ACD-crosslinked actin oligomers potently inhibit Ena/VASP-mediated actin polymerization

Undergraduate Research Thesis

Presented in Partial Fulfillment of the Requirements for graduation "with Honors Research Distinction in Biochemistry" in the undergraduate colleges of The Ohio State University

By

Kyle E. Shafer

The Ohio State University

May 2016

Project Advisor: Dr. Dmitri Kudryashov, Department of Chemistry and Biochemistry

Table of Contents

Abstract

The actin crosslinking domain (ACD), a product of pathogenic Gram-negative bacteria *Vibrio cholera*, *Vibrio vulnificus* and *Aeromonas hydrophila*, is a potent, actin-specific toxin. Once in the cytoplasm of host cells, ACD catalyzes the intermolecular, amide bond formation between the actin residues glutamic acid-270 and lysine-50 in two different actin monomers. This crosslinking leads to the formation of non-polymerizable actin oligomers and eventual cell rounding. Recently, our laboratory found that actin oligomers potently inhibit formins, a family of actin binding proteins that regulates many actin-dependent processes. This potency of actin oligomers is achieved by binding with high affinity to tandemly organized G-actin-binding domains in formins, an attribute enabled by binding to multiple sites on the formins. Similarly, it is possible that actin oligomers may affect other actin regulatory proteins that have several actin-binding domains organized in close proximity. Ena/VASP is such an actin regulatory protein, which increases the rate of actin polymerization approximately two to three fold. Previously, Ena/VASP had not been identified as a target of bacterial toxins.

To study the effects of actin oligomers on Ena-controlled actin polymerization, we employed pyrene polymerization assays. A potent, dose-dependent inhibition of Ena by oligomers was observed both in the presence and absence of profilin, a major regulator of polymerization of actin monomers. We also determined that profilin does not play a significant role in the inhibition mechanism. These results suggest that the mechanism of filament growth inhibition is similar to that of a capping protein where the inhibition occurs once Ena is already associated with the actin filament. The observation of single filament growth in the presence of Ena and oligomers will help to confirm this mechanism. Further understanding of the role of ACD-crosslinked actin oligomers will allow us to create tools to study and control Ena/VASP-mediated processes.

Acknowledgements

As a member of the Kudryashov Laboratory at The Ohio State University Department of Chemistry and Biochemistry for four years, I have received extensive instruction and guidance from great mentors that have made my work in this thesis possible. I would first like to thank my principal investigator, Dr. Dmitri Kudryashov, for welcoming me into his laboratory, providing me with all the tools necessary to carry out my project, as well as mentoring me, challenging me, and encouraging me throughout my research. He is very driven and professional, and he greatly cares about the success of the members of his laboratory. Additionally, I would like to thank Dr. Elena Kudryashova, a research scientist in the lab, for her intellectual guidance, support, and mentorship throughout my research. I would also like to thank David Heisler, a graduate student in the Kudryashov Lab, who has been a great trainer of countless laboratory techniques, provider of assistance with experimental design and result analysis, and instructor of numerous biochemical concepts used during my research. Finally, I would like to thank all other members of the Kudryashov Lab for the valued intellectual and technical assistance they have provided me over the course of the past four years.

1. Introduction

1.1 Bacterial toxins and their cellular effects

Bacterial toxins are the deadliest compounds on Earth; single copies of some toxins are sufficient to kill an entire host. In general, toxins are able to be so efficient by targeting proteins that are essential for survival of the host (e.g. inhibition of protein synthesis by the diphtheria toxin (1)) or by acting on signal transduction cascades (e.g. modification of the G-Coupled Protein Receptor signaling cascade (2)). Conversely, actin, a major component of a host's cytoskeleton, is often a target of bacterial toxins through direct modification (3). Because actin is one of the most abundant proteins in the cell, with concentrations exceeding 100 μM (4), it was unclear until recently how actin specific toxins could achieve such high efficiency.

1.2 Cellular roles of actin

Actin is a 42 kDa, ubiquitously expressed protein found in all eukaryotic cells. In the cell, actin exists in equilibrium between monomeric actin (G-actin) and filamentous actin (F-actin); under appropriate conditions, G-actin can polymerize to form F-actin and F-actin can depolymerize into G-actin. Actin serves numerous roles within the cell: it allows cells to alter their shape, divide, exo- and endocytose, and be motile (6). Accordingly, actin serves significant roles in host immunity. The actin cytoskeleton allows the immune system to carry out many of its necessary functions such as migration, phagocytosis, B and T cell activation, secretion, and cell-cell interactions (7). To carry out these roles, actin functions in association with many other proteins that regulate the dynamic equilibrium to increase or decrease the rate of polymerization and elongation and assist in forming higher-order actin assemblies (e.g., branched networks and bundles of filaments) (6).

1.3 Actin-specific toxins

Since actin plays many important roles in host immunity, it is not surprising that pathogens have developed a way to compromise the structure and function of the actin cytoskeleton and/or utilize the actin cytoskeleton for their advantage. One way that bacteria can manipulate the actin cytoskeleton is through the production of toxins. Bacterial toxins effecting actin typically fall in one of three groups: those that nucleate actin and increase the F-actin pool while decreasing the G-actin pool, those that sequester G-actin and increase the G-actin pool while decreasing the F-actin pool, and those that activate or inactive Rho GTPases. Activation of Rho GTPases increases the polymerization of actin. Through the interaction between the host Arp2/3 complex and the ActA protein on *Listeria monocytogenes*, Act A causes the nucleation of G-actin and a shift in the equilibrium towards F-actin (8). The *Clostridium botulinum* C2 toxin, *Salmonella enterica* SpvB toxin, and *Clostridium perfringens* iota toxin cause ADP-ribosylation of actin at arginine-177, which inhibits its polymerization (3). The bacterial toxins from *Clostridium difficile*, *Clostridium sordellii*, and *Clostridium novyi* inactivate Rho family proteins through glycosylation, while the necrotic factor from *Escherichia coli* activates Rho by deamidation (2).

1.4 ACD catalyzes formation of covalent actin oligomers

The actin crosslinking domain (ACD) does not modify actin like all other known bacterial toxins. ACD depletes the pools of both G- and F-actin, unlike the toxins mentioned previously. ACD is an actin-specific toxin found within the larger group of MARTX and VgrG1 toxins found in Gram-negative bacteria from some *Vibrio* and *Aeromonas* species (9). Once delivered to the cytoplasm of the host cell, ACD catalyzes the intermolecular amide bond formation between the actin residues glutamic acid-270 (E270) and lysine-50 (K50), leading to

the formation of various size actin oligomers (10). K50 is located on subdomain 2 of an actin monomer while E270 is located on subdomain 3. When the amide bond forms between the residues, it causes a twist in subdomain 2 that disrupts the normal inter-subunit interface between actin monomers during the formation of an actin filament, resulting in its inability to polymerize (Figure 1) (10). ACD converts monomeric actin into cross-linked actin oligomers, decreasing both the monomeric and filamentous actin pools (11) and leading to the loss of critical functions such as motility, contractility and rigidity (12). *In vivo*, the addition of oligomers results in the disassembly of actin stress fibers and cell rounding (13).

1.5 Oligomer toxicity and actin-regulatory proteins

Until recently, the accepted hypothesis of ACD toxicity was the bulk accumulation of ACD–crosslinked actin oligomers (14). Given the high concentration of actin within the cell (>100 μM) and the rate of single molecule ACD-mediated acting crosslinking (15), it was previously determined that it would take over six months for a single ACD molecule per cell to crosslink half the actin cytoskeleton (9). The vast amount of actin within the cell would seem to make ACD a very inefficient toxin. Yet, our lab recently found that relatively low amounts of intracellular cross-linked oligomers (2-6%) caused a dramatic change in cell morphology, indicating that the oligomers likely play an active role in toxicity (9). The oligomers possess a unique and toxic combination of properties found in neither F- nor G-actin: unlike F-actin, they can bind G-actin binding proteins (e.g. profilin and thymosin-β4), but unlike G-actin, the oligomers contain multiple binding sites for such proteins. It was hypothesized that these unique characteristics would allow the oligomer to bind to tandem-organized actin binding domains of key actin assembly factors such as formins (9). Formins are homo-dimeric proteins characterized by their formin-homology 1 and 2 domains (FH1, FH2). The FH1 domains are made up of

multiple poly-proline rich regions in tandem, each capable of binding actin monomers in complex with the G-actin binding protein profilin. The FH2 domain forms a homodimer that stays processively attached to the barbed end of a growing actin filament. Binding of actin-profilin complexes to the FH1 domains increase a local concentration of polymerization-competent actin monomers and feed the FH2 domain with G-actin to increase the rate of filament elongation by 5-10 fold (16). When actin oligomers were introduced into *in vitro* actin polymerization assays, they exhibited a dose-dependent inhibition on formin-mediated actin elongation (9).

Formins are not unique in having multiple actin binding domains. In fact, a majority of proteins that regulate the actin cytoskeleton have several actin-binding domains in proximity (either in tandem or due to oligomerization (17)). Therefore, it is likely that more than just the formin family of proteins that are targeted by the actin oligomers. One candidate is the Ena/VASP family of proteins, a filament assembly factor.

1.6 Ena/VASP protein family

The Ena/VASP family of proteins are found across a wide variety of eukaryotes and share the same structural domains (18). For example, *Dictyostelium discoideum* expresses DdVASP, *Drosophila* expresses Ena (Enabled), and mammals express EVL (Ena/VASP-like), Mena (mammalian Ena), and VASP (vasodilator-stimulated phosphoprotein) (18). *In vivo*, Ena/VASP proteins gather and promote elongation of lamellipodial actin-barbed ends as well as antagonize the inhibition of polymerization by capping protein. As an active tetramer, Ena/VASP can stay processively attached to the growing actin filament (19). Mice and *Drosophila* studies indicate that Mena and Ena function in the axonal architecture of both the central and peripheral nervous system, respectively (18). VASP is involved in numerous processes including platelet

aggregation, as VASP deficient mice exhibit defects in the actin-dependent process of platelet aggregation (12).

While different members of the Ena/VASP family slightly vary in their structure and amino acid composition, they all form tetramers and therefore contain several G-actin binding domains in close proximity. This allowed us to focus on Ena alone as a representative member of the family that can be expressed in bacteria. Therefore, conclusions from the work presented here can be extended into the human model (20). Like all other members of the family, Ena contains an Ena/VASP homology domain 1 (EVH1), a polyproline-rich region and EVH2 domain (Figure 2). In its active form, Ena exists as a tetramer, which is largely facilitated by its coiled-coil domain in EVH2 (18). This tetramerization allows Ena to increase the elongation rate of actin between two to three-fold (19). Additionally, there is a linker between the EVH1 and polyproline-rich region of unknown function. Deletion of this linker (Ena(ΔL)) has also been shown not to effect the elongation rate of Ena-controlled actin filaments *in vitro*. It is likely this linker region is important for localization and appropriate function *in vivo*. Also, because Ena(ΔL) has a higher protein yield upon expression in *E. coli* and is more active after long-term storage at -80 °C as compared to the full length protein (19), it was utilized in all experiments completed for this thesis.

1.7 Functional roles of the EVH1 domain and polyproline-rich regions

The first 115 residues of the Ena protein is the EVH1 domain. These residues play important roles in forming links to host proteins that contribute/regulate various signal transduction pathways. EVH1 is a non-catalytic protein interaction domain that specifically binds to target proline-rich (FPPPP-containing) sequences. These sequences are found in mammalian proteins including the focal adhesion proteins zyxin and vinculin as well is in the ActA protein

for the pathogen *Listeria monocytogenes*. In general, the binding to the FPPPP sequences has a low affinity and high specificity in order to carry out successful signaling cascades (21).

Another highly conserved region in the Ena/VASP family is the polyproline-rich region. Through analysis of the distribution of hydrophobic amino acid clusters, three distinct groups of proline residues were observed in all members of the Ena/VASP family. It is hypothesized by Ferron et al. that each of these groups has their own specific role in Ena function to bind profilin-actin complexes, the major pool of polymerization competent actin within eukaryotic cells (22). The first polyproline rich region is termed the regulatory region and consists of a mixture of proline and hydrophobic amino acids. This mixture is a feature of SH3 (SRC Homology 3) and WW-binding sequences that are located on a number of signaling proteins. This site does not correspond to a profilin-binding sequence and is likely involved in regulation by SH3 proteins. The next region is termed the recruiting site as it contains three repeats of the specific profilin-binding sequence GPPPPP and can subsequently bind multiple profilin-actin complexes. The final region is the loading site, which is highly conserved among all members of the Ena/VASP family (22). This site is located between the recruiting site and EVH2. It is flanked by short flexible glycine linkers and participates in delivering profilin-actin from the polyproline-rich region to the EVH2. Tentatively, profilin-actin can move from region to region toward the EVH2 domain due to increasing affinity to each subsequent site (22).

1.8 Function of the EVH2 domain

The C-terminal portion of the protein is the highly conserved EVH2 domain, made up of the G-actin binding domain (GBD), the F-actin binding domain (FBD) and the coiled-coil motif. The KLKK sequence of the G-actin binding domain resembles a motif in thymosin-β4, an actin monomer-binding protein (23). This binding site contacts the gelsolin- and profilin-binding sites

on the barbed end of actin monomers without blocking the DNAseI binding on subdomain 2 of the monomer (24). The FBD can bind and bundle F-actin (18). Coordination between the G-actin binding domains and F-actin-binding domains in the tetramer allows Ena to stay processively attached to the filament. The FBD binds to the sides of the filament, tethering the tetramer near the barbed end, and GBD binds to G-actin or, F-actin with lower affinity (Figure 11), to deliver actin monomers to the filament. Before one Ena peptide dissociates from the filament, any of the other peptides in the tetramer can bind to adjacent actin protomers and add a monomer, allowing for the processivity of the protein (19).

1.9 Thesis overview

There were three primary goals for the work completed in this thesis. The first was to express and purify the active Ena(ΔL) construct. After this was completed, the next focus was to determine if ACD-crosslinked actin oligomers would inhibit Ena(ΔL)-mediated actin polymerization. This was entirely assessed through pyrene-actin polymerization assays. Since there is an inhibitory effect, the final goal was to determine how the oligomers are gaining their inhibitory effect. By changing the order of addition of actin oligomers, we gained an insight into the mechanism of oligomer inhibition. This goal still needs further experimentation looking at oligomer inhibition at a single filament level to confirm our model.

In the following chapters, I will explain the implication of my results and discuss some of my project's challenges. Subsequently, I will propose a mechanism, future directions, and discuss the potential significance of this project on the importance of the study of ACD-crosslinked actin oligomers. Finally, I will describe detailed methodology for Ena(ΔL) expression and purification, the formation of ACD-crosslinked actin oligomers, and the use of pyrene-actin polymerization assays.

2. Results

2.1 Ena expression and characterization

Active Ena(ΔL) was successfully expressed using *E. coli* Codon Plus® cells and purified as described in "Methods". Codon Plus® *E. coli* were selected since they are engineered to contain extra copies of genes that encode rare tRNAs in *E. coli* that are more abundant in sophisticated organisms, such as *Drosophila*. Purification was assessed using SDS-PAGE and was determined to be sufficiently pure without further purification steps necessary (Figure 3). The N-terminal maltose binding protein and C-terminal His tags were not cleaved from the protein as they were previously shown not to effect Ena(ΔL) activity (19). To assess the activity of the purified protein, we utilized pyrene actin polymerization assays to monitor polymerization of actin alone or in the presence of Ena(ΔL) (Figure 4). Ena(ΔL) increased the polymerization rate compared to actin alone (Table 1). In comparing the approximate elongation rate at ~50% of max polymerization (Figure 4A, Table 1), enhancement of polymerization plateaued at approximately 20 nM of Ena(ΔL), about a two-fold increase in the filament elongation rate compared to non-Ena(ΔL) controlled filaments.

Ena(ΔL) concentration (nM):	Elongation rate without PFN1 (μM/s) (Figure 4A):	Relative increase in elongation rate without PFN1:	Elongation rate with PFN1 (μM/s) (Figure 4B):	Relative increase in elongation rate with PFN1:
0	0.00091	1.0	0.00075	1.0
10	0.00158	1.7	0.00106	1.4
20	0.00173	1.9	0.00165	2.2
40	0.00189	2.1	0.00166	2.2

Table 1: Elongation rate analysis of polymerization traces in Figures 4A and 4B.

Another way to look at the elongation rate increase by Ena(ΔL) is to compare the time it takes for each trace to reach half of its maximum polymerization at each concentration of

Ena(ΔL). The time to half maximum includes a waiting time that depends on the number of seed filaments that are nucleating spontaneously from monomers. Since Ena(ΔL) is not an actin nucleator (25), this should be the same at all concentrations of Ena(ΔL) and the actin control. In agreement with previous data (19), this data, shown in Table 2, also indicates that Ena(ΔL) increased the polymerization rate as compared to actin alone. Even though the results obtained by the two methods are overall very similar, in the latter case the rate enhancement of polymerization slightly increased between 20 and 40 nM of Ena(ΔL) suggesting either weak nucleation activity of Ena, or some other details in the activity of Ena that we do not fully understand. This further suggests that comparing time to half maximum polymerization is a more sensitive way of assessing the effects of Ena.

Ena(ΔL) concentration (nM):	Time to half max polymerization without PFN1 (s) (Figure 4A):	Relative times faster in reaching half max polymerization without PFN1:	Time to half max polymerization with PFN1 (s) (Figure 4B):	Relative times faster in reaching half max polymerization with PFN1:
0	1808.6	1.0	4358.6	1.0
10	1223.5	1.5	2723.6	1.6
20	938.5	1.9	2363.5	1.8
40	788.5	2.3	2093.5	2.1

Table 2: Time to half maximum polymerization for the polymerization traces in Figures 4A and 4B.

Additionally, we tested activity in the presence of human profilin-1 (PFN1), and found that Ena(ΔL) was still able to increase the bulk rate of actin polymerization (Table 1,2). Similarly, enhancement of elongation plateaued at 20 nM of Ena(ΔL) for the data in Table 1, however, when looking at the time to half maximum polymerization (Table 2), the rate enhancement of polymerization again increased between 20 and 40 nM of Ena(ΔL). Both analyses of rate agreed on a two-fold increase compared to non-Ena(ΔL) controlled filaments.

Because Ena(ΔL) does not nucleate filaments at physiological salt concentrations (25), the addition of PFN1 did not significantly enhance the activity of Ena (Figure 4) in contrast to formins where profilin-actin complexes accelerated elongation by as much as 10-fold (9). This can be observed in the similar elongation rates at the same Ena(ΔL) concentrations in both the absence and presence of PFN1. In both the absence and presence of PFN1, the rate enhancement plateaued at approximately 20 nM of Ena(ΔL). Therefore, all subsequent assays utilized 20 nM of Ena(ΔL) to test the effects of actin oligomers.

2.2 Actin oligomers inhibit Ena-controlled filament elongation in a dose dependent manner

It has been previously shown that actin oligomers have only a marginal effect on spontaneous actin polymerization in the absence and presence of PFN1 (9). When ACD-crosslinked oligomers were mixed with Ena(ΔL) and actin, there was a potent decrease in the polymerization rate as the concentration of oligomers increased (Figure 5). To determine the median inhibitory concentration (IC_{50}) of the oligomers, we determined the tangent slope of each curve at 50% (linear intervals of polymerization curves at 40-60% were assessed) in polymerization assays. Fitting the inhibition to an isotherm binding equation yielded an IC_{50} of 3.70 ± 0.95 nM (Figure 6), suggesting that the oligomers are nearly as efficient in inhibition of Ena as in that of mDia1, a formin that was previously shown to be potently inhibited by the oligomers (9). High concentrations of the oligomers (> 100 nM) caused a mild reversal in inhibition. A likely interpretation of this effect is weakening of the filaments upon incorporation of a small fraction of the oligomers. Such weakening can result in filament severing leading to the generation of additional filament ends capable to participate in elongation and thus to contribute to overall faster polymerization (Figure 5) (9).

2.3 Profilin does not play a major role in the oligomer inhibitory mechanism

In cells, most of the G-actin pool is bound to profilin to inhibit spontaneous nucleation and regulate actin interaction with numerous filament assembly factors (6). In the presence of profilin, the addition of the oligomers showed a potent decrease in the bulk polymerization rate (Figure 7), of similar efficiency to that observed in the absence of profilin. An IC_{50} value of 3.21 ± 0.53 nM (Figure 6) was obtained, indicating that profilin does not play a role in the oligomers inhibition mechanism. There was not the reversal in potency of inhibition at high concentration of the oligomers as observed without profilin (Figure 7). This is because profilin inhibits incorporation of the oligomers into growing filaments (9).

2.4 Oligomers inhibit Ena that is already associated with the growing filament

To gain insight into how the oligomers were achieving their inhibitory effect, the oligomers were added to Ena-controlled actin filaments. To generate Ena(ΔL)-controlled filaments, actin was polymerized in the presence of Ena(ΔL) and at approximately 15% of maximum polymerization, different concentrations of oligomers were added. A dose-dependent inhibition was observed as in the previous assays where oligomers were added before polymerization (Figure 8). If inhibition was only occurring by oligomer binding to Ena(ΔL) prior to association with the filament, the polymerization curves at all concentrations of oligomers would be unaffected. However, our results indicate that the oligomers are capable of bind to Ena(ΔL) that is associated with elongating filaments. Fitting the inhibition to the isotherm binding equations resulted in an IC_{50} of 5.80 ± 0.69 nM (Figure 9).

The role of profilin in the inhibition mechanism was also assessed though the addition of oligomers to Ena controlled filaments in the presence of PFN1. Similarly, there was a dose

dependent inhibition of Ena(ΔL)-mediated polymerization (Figure 10). With an IC50 value of 2.73 ± 0.45 nM (Figure 9), we found that profilin may play a role in recruiting the oligomers.

3. Discussion

Many proteins play an active role in controlling actin dynamics. When these accessory proteins are inhibited or do not function normally, cellular processes can be greatly impacted. ACD is a bacterial toxin that works by producing toxic actin oligomers to inhibit these accessory proteins. Our goal is to understand which actin-binding proteins are affected by the oligomers, and apply this knowledge to develop novel tools for studying the actin cytoskeleton. Our results are the first example of Ena serving as a target for bacterial toxins.

Actin oligomers in the presence or absence of profilin have a dose-dependent inhibition of Ena. This inhibition is likely to be accountable, at least in part, for the observed cell rounding in cells treated with ACD. The mechanism by which the oligomers gain their inhibitory power is only partially understood (Figure 11). Ena, as an active tetramer, has multiple G-actin binding, F-actin binding and poly-proline rich domains in close proximity (Figure 11, 13). The four F-actin binding domains allow for a walking action of the protein to stay processively attached to the barbed end of the growing actin filament (19). We propose that the four proximal G-actin binding domains provide a platform for multivalent, high affinity binding of the oligomers, which potently prevents further polymerization. Since the surface on actin that interacts with the G-actin binding domain of Ena is not altered by the ACD crosslink, the oligomers should be capable of binding to this domain. However, the crosslink induces a change in the monomer orientation that inhibits the formation of appropriate contacts within the growing filament; thus elongation stalls and Ena is converted into a filament capping protein.

Interestingly, the addition of profilin does not seem to have a major effect on the affinity of oligomers to Ena. The efficiency of inhibition is similar in polymerization assays where the oligomers were pre-mixed with Ena prior to the initiation of polymerization (and therefore had a chance to inhibit Ena in solution) or added after initiation of polymerization (when Ena is bound

to the filament barbed ends). This suggests that the active, filament-bound form of Ena is a target of the oligomers. There is a slightly stronger affinity for oligomers to Ena in the presence of PFN1 in seeded assays, possibly indicating that profilin helps to recruit oligomers through the interaction with the poly-proline rich domain in Ena, similar to what was found for formins (9). However, this recruitment plays only a minor role.

While homologous to VASP, Ena is a *Drosophila* protein. In our assays, we used the human homolog of profilin, PFN1, rather than *Drosophila* profilin Chickadee. In an alignment allowing for gaps in the proteins, there is a 25% identity and 50% similarity between Chickadee and human profilin (26). It is not known if PFN1 is capable of binding to Ena, and therefore may explain our observation of profilin playing only a small role. Based on the similarity percentage, however, it is likely there will not be a difference when using Chickadee. Future experiments should still be done with Chickadee to confirm the results.

Our results indicate that the oligomers bind to and inhibit Ena after Ena associates with an actin filament. We confirmed that filaments previously elongating by Ena are potently inhibited by the addition of the oligomers. This can be confirmed using TIRF microscopy and looking at single actin filament growth controlled by Ena. It is also possible that the oligomers can bind only to free Ena in solution, however if this were the case, the addition of oligomers to the Ena-controlled polymerizing filaments should have resulted in no effect on the polymerization. Ena bound to oligomers can associate with the filament based on our spontaneous polymerization results.

While future research is necessary in order to completely understand how the oligomers inhibit the polymerization rate enhancement of Ena-associated filament growth, a few important results have arisen from the work completed for this thesis. We learned that Ena(ΔL) is an

indirect target (through the produced oligomeric actin species) for bacterial toxins, specifically ACD in this case. Given that the inhibition of Ena by the oligomers is largely profilin-independent, this indicates that the effect is mediated via oligomers binding to the WH2-domain of Ena. Therefore, this study is the first example that the ACD-crosslinked oligomers can target WH2-domain actin binding proteins (e.g. the GBD of Ena). These results strongly suggest that many other actin regulatory proteins containing tandem WH2-actin binding domains (i.e. Spire, Cobl, nucleation promoting factors assisting the activation of the Arp2/3 complex, etc.) are likely to be affected by actin oligomers. Finally, since we have found that ACD-crosslinked actin oligomers have a high affinity for Ena(ΔL), we can now utilize them to further study and control Ena/VASP mediated processes.

4. Materials and Methods

4.1 Protein purification

4.1.1 Actin

Actin was prepared from acetone powder of rabbit skeletal muscle (Pel-Freeze Biologicals) as previously described (27), gel filtered, stored on ice in G-buffer (5mM Tris-HCl, pH 8.0, 0.2 mM $CaCl_2$, 0.2 mM ATP, and 5 mM β-mercaptoethanol (βME)), and used within two weeks.

4.1.2 ACD

Thermo-labile ACD from *Aeromonas hydrophila* (ACD_{Ah}) was utilized as it can be inactivated under mild heating conditions that do not denature the oligomers themselves. The enzyme was expressed and purified as previously described (28).

4.1.3 Ena(ΔL)

Ena(ΔL), a construct containing EVH1, poly proline region, EVH2 and a coiled-coil domains (residues 1-112 and 297-684) in a pET21a-MBP(TEV) vector with N-terminal maltose binding protein (MBP) and C-terminal 6xHis tags, was a gift from Dr. David Kovar (University of Chicago). This construct was expressed in *E. coli* BL21 CodonPlus® competent cells in a rich bacterial cell growth medium (1.25% tryptone, 2.5% yeast extract, 1 mM proline, 125 mM NaCl, 0.4% glycerol, and 50 mM Tris-HCl, pH 8.2). Expression was induced by the addition of 1 mM IPTG. Cells were incubated overnight at 16 °C before centrifugation. Cell pellets were resuspended in extraction buffer (50 mM NaH_2PO_4, pH 8.0, 0.5 M NaCl, 10% glycerol, 10 mM imidazole, 0.02 mg/mL LP, 0.02 mg/mL Trypsin inhibitor, 4 mM benzamidine, and 1 mM PMSF). Cells were lysed via sonication, and following clarification by centrifugation, the lysate was incubated with Talon® cobalt metal affinity resin (Clontech), washed extensively with lysis

buffer, and eluted with buffer containing 50 mM NaH_2PO_4, pH 8.0, 0.5 M NaCl, 10% glycerol, 0.1 mM PMSF, and 250 mM imidazole. Samples containing Ena(ΔL), as detected by SDS-PAGE, were dialyzed against storage buffer (20 mM HEPES, pH 7.4, 200 mM KCl, 0.01% NaN_3, and 1 mM DTT). Ena(ΔL) was flash-frozen in liquid nitrogen and stored at -80 °C. The concentration of Ena(ΔL) was determined by comparing protein bands of various dilutions of Ena(ΔL) to protein bands of known actin concentration on a 7.5% SDS-PAGE gel.

4.1.4 Human profilin 1 (PFN1)

PFN1 was expressed in *E. coli* BL21 Codon Plus® competent cells in a rich bacterial growth medium and was purified on poly-L-proline sepharose resin as previously described (29). Purified profilin was dialyzed against three storage buffer changes (2 mM Tris-HCl, pH 8.0, 0.2 mM EGTA, 1 mM DTT, and 0.1 mM PMSF) before flash freezing at -80°C.

4.2 ACD-crosslinked actin oligomer preparation

Monomeric actin was first diluted to 20 μM in reaction buffer (5 mM HEPES, pH 8.0, 0.2 mM ATP, and 0.1 mM PMSF) and mixed with 10 nM ACD_{Ah} and 1 mM $MgCl_2$ to begin the crosslinking reaction, which was allowed to proceed for 45 min at 10°C. The reaction was terminated by heat inactivation at 42°C for 20 min. To remove uncrosslinked actin, the concentration of $MgCl_2$ was brought to a final concentration of 3 mM and the sample was incubated at 25°C for 30 min to allow the non-crosslinked actin species for fully polymerize. The non-crosslinked actin, now polymerized, was removed by centrifugation at 300,000 g for 30 min at 4°C using a TLA-100 rotor in an Optima TL-100 ultracentrifuge (Beckman Coulter). The supernatant containing the actin oligomers was supplemented with 1 mM ATP and used in less than one week.

4.3 Actin labeling with pyreneiodoacetamide

Pyrene-labeled actin was prepared as previously described (30).

4.4 Actin polymerization assays

Gel-filtered Ca^{2+}-ATP G-actin (5% pyrenyl-labeled; 2.5 μM final concentration) was pre-mixed in black 384-well plates with 20 nM of Ena(ΔL), varying (0-200 nM) concentrations of actin oligomers, and with and without 5 μM PFN1 (all concentrations are given as final) in the reaction buffer (10 mM MOPS, pH 7.0, 0.2 mM ATP, and 0.5 mM DTT). Then, Ca^{2+}-ATP G-actin was converted to Mg^{2+}-ATP G-actin by adding 0.066 volumes of switch buffer (150 mM MOPS, pH 7.0, 3 mM ATP, 7.5 mM DTT, 4.5 mM EGTA, and 1.5 mM $MgCl_2$) and incubating at room temperature for 1 min. Polymerization was initiated by adding 0.33 volumes of initiation buffer (30 mM MOPS, pH 7.0, 0.6 mM ATP, 1.5 mM DTT, 150 mM KCl, and 3 mM $MgCl_2$). Pyrene fluorescence was monitored at λ_{ex} = 365 nm and λ_{em} = 407 nm using an Infinite M1000 Pro plate reader (Tecan).

Assays where oligomers were added at ~15% max polymerization were completed using the same method as described for actin polymerization assays. After approximately 200 s and 960 s for without PFN1 and with PFN1, respectively (~ 15% max polymerization), 0.066 volumes of varying (0-200 nM) concentrations of actin oligomers were added and pyrene fluorescence monitoring was resumed. The oligomers were not pre-mixed with Ena and with and without PFN1.

4.5 Data analysis

Inhibition of polymerization by actin oligomers was assessed through the calculation of the tangent slope of each pyrene fluorescence trace at 50% (linear intervals of polymerization

curves at 40-60% were assessed) of maximum polymerization. The obtained inhibition was fitted to a binding isotherm equation using Origin software (OriginLab):

$$\frac{\Delta F}{\Delta F_{max}} = \frac{M+X+IC_{50}-\sqrt{(M+X+IC_{50})^2-4\cdot M\cdot X}}{2\cdot M} \quad \textbf{(1)}$$

where M = Ena(ΔL) concentration, X = concentration of crosslinked actin oligomers, IC_{50} = the oligomer concentration causing 50% inhibition of Ena(ΔL) activity, ΔF = the observed pyrene fluorescence change, and ΔF_{max} = the maximum pyrene fluorescence change.

The error bars on the IC_{50} plots are an indication for the variance in each data set. In each plot, three sets of data were combined and the marker indicates the average value at each concentration of the three sets. The isotherm binding equation was then fit to these average points and the resulting deviation is based on the fit of the curve to these averages.

5. Figures

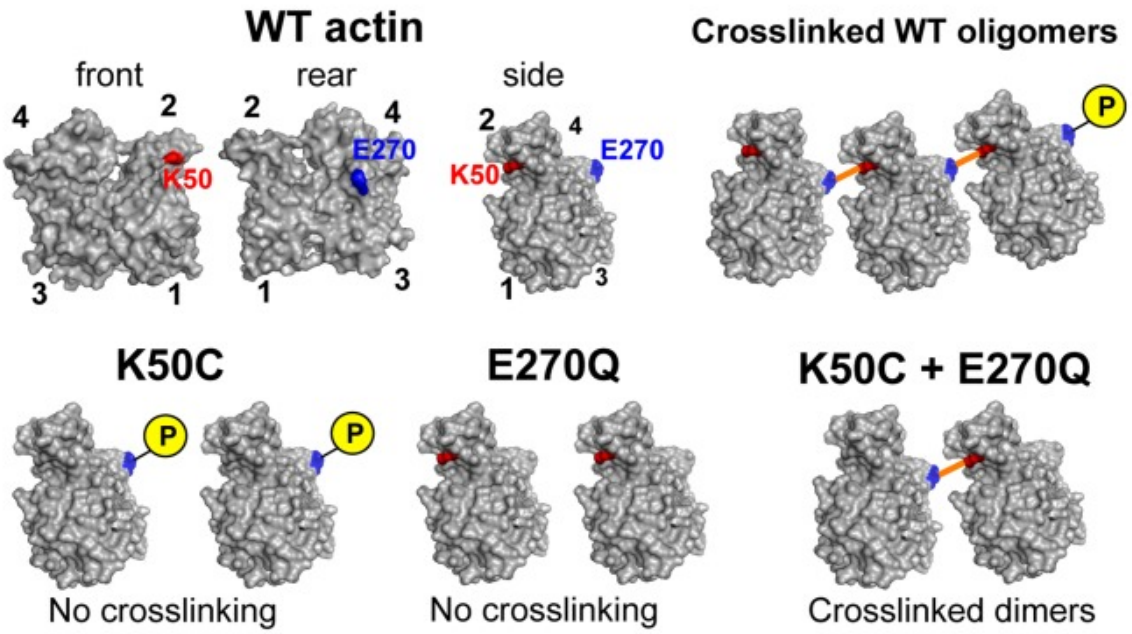

Figure 1: Crosslinked actin oligomers have a twist in subdomain 2 that disrupts the normal inter-subunit interface between actin monomers during the formation of an actin filament, resulting in its inability to polymerize. The P indicates a phosphate group, as the formation of glutamyl phosphate is an intermediate and activation step of the ACD catalysis. Adapted from *Kudryashova et al., PLoS One, 2012* (10).

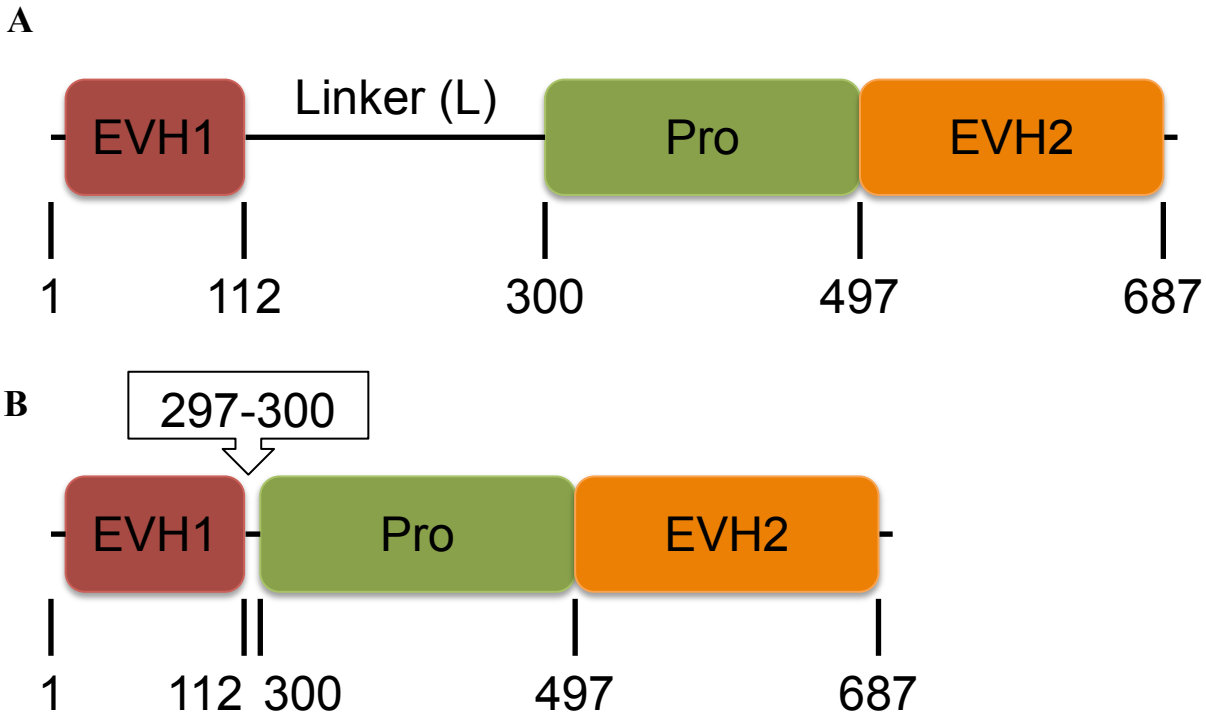

Figure 2: A) Full-length Ena with linker region. **B)** Ena(ΔL) construct with the linker region removed. Numbering represents amino acids. Both constructs have an N-terminal MBP and C-terminal His_6 tag that were not removed after purification since they did not have an effect on activity (15).

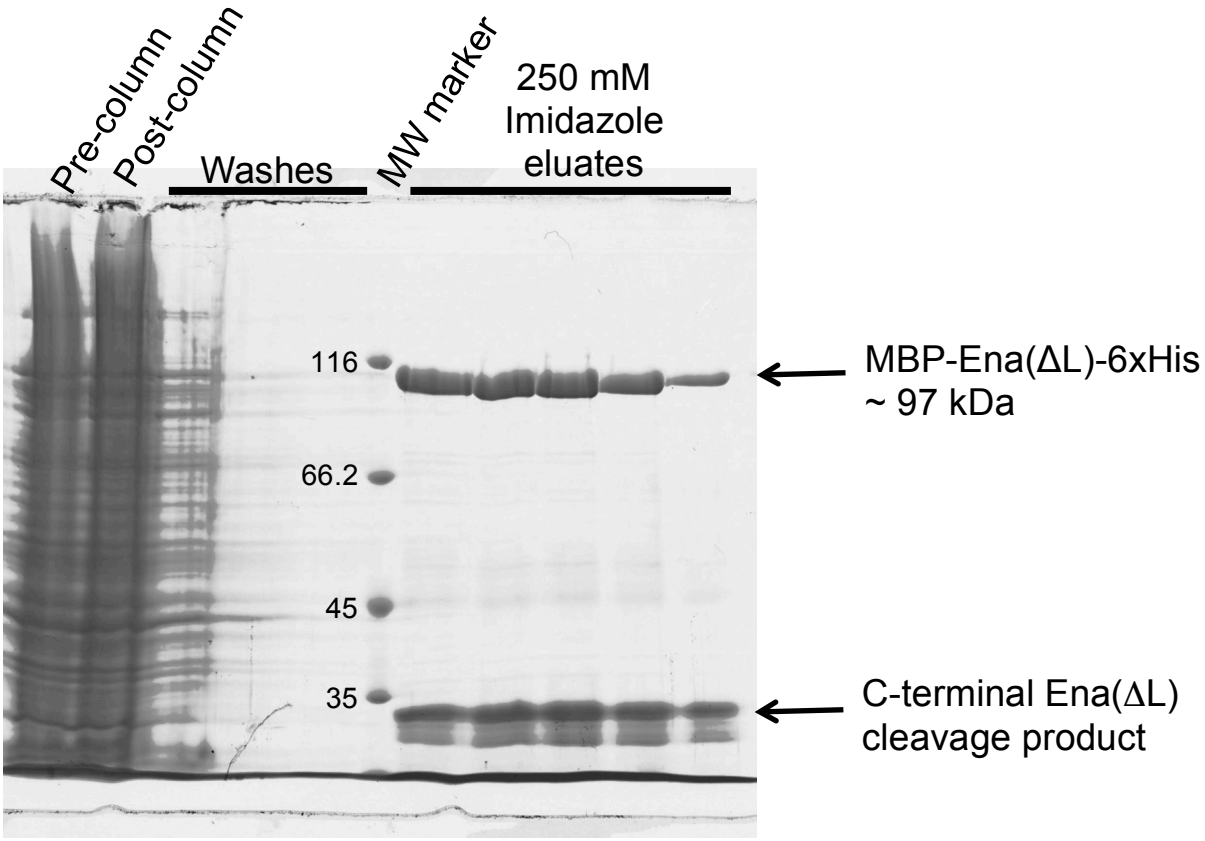

Figure 3: SDS-PAGE of Ena(ΔL) purification. Ena(ΔL) was purified via metal affinity chromatography. Molecular weights indicated for the marker lane.

A

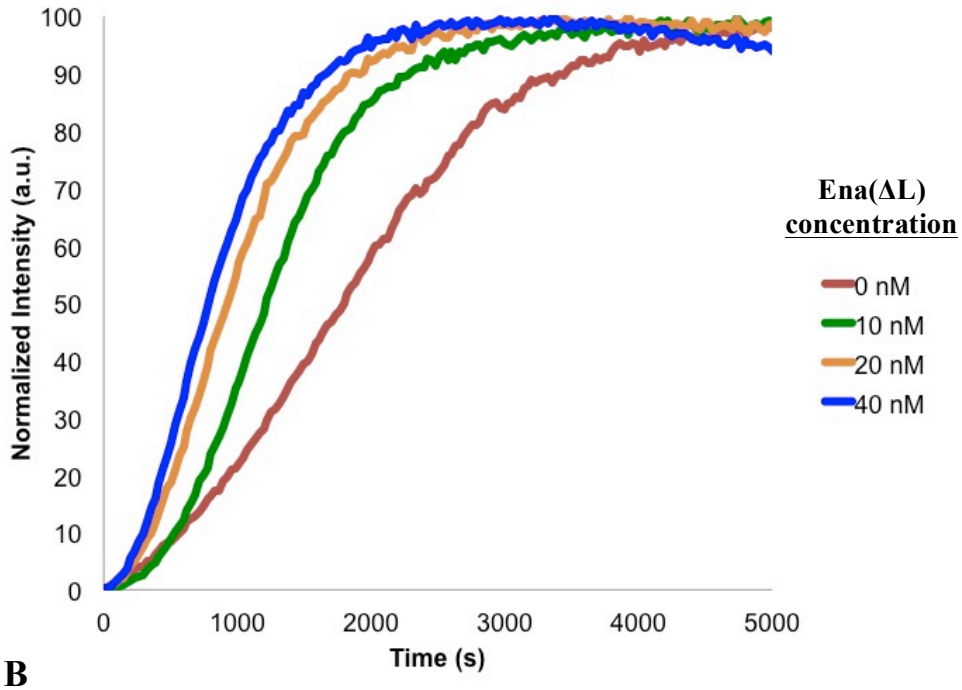

B

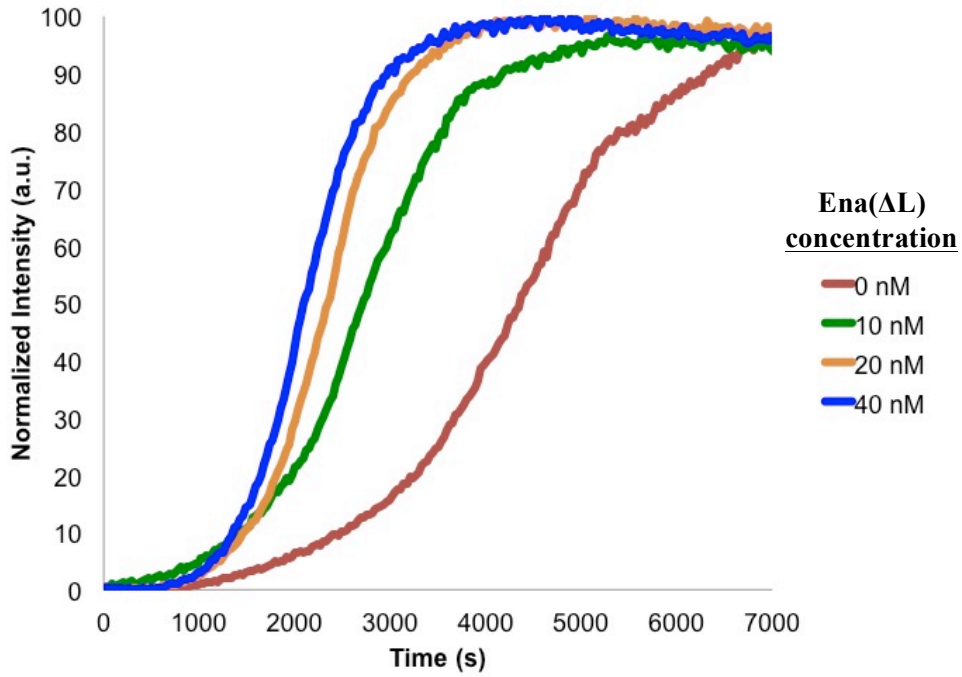

Figure 4: Effects of various Ena(ΔL) concentrations on polymerization of 2.5 μM actin in the absence **(A)** and presence **(B)** of 5 μM PFN1.

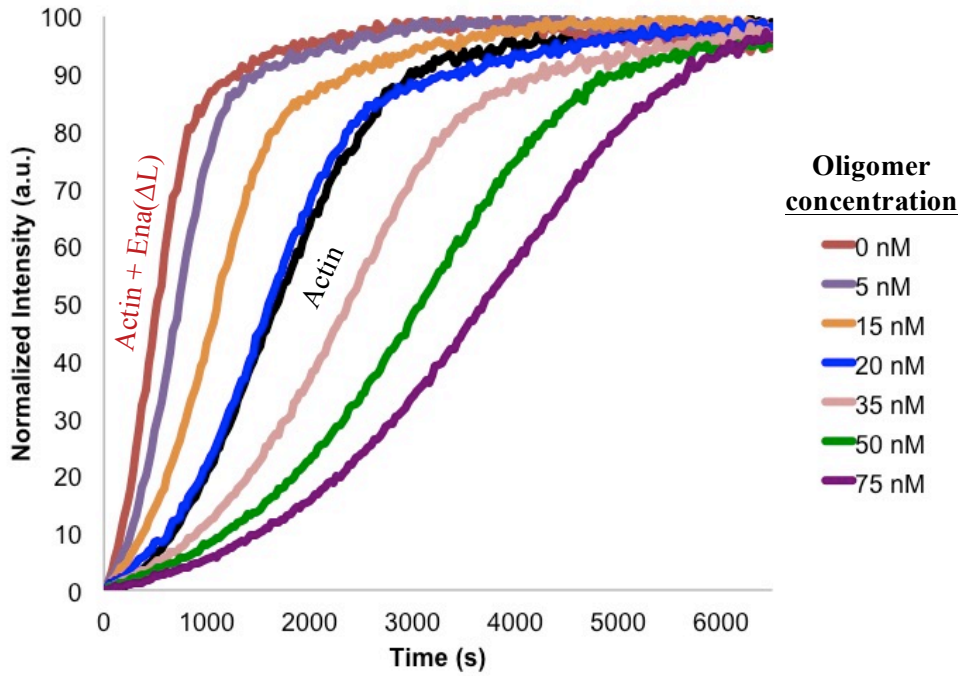

Figure 5: Effects of various oligomer concentrations on polymerization of 2.5 µM actin mediated by 20 nM Ena(ΔL).

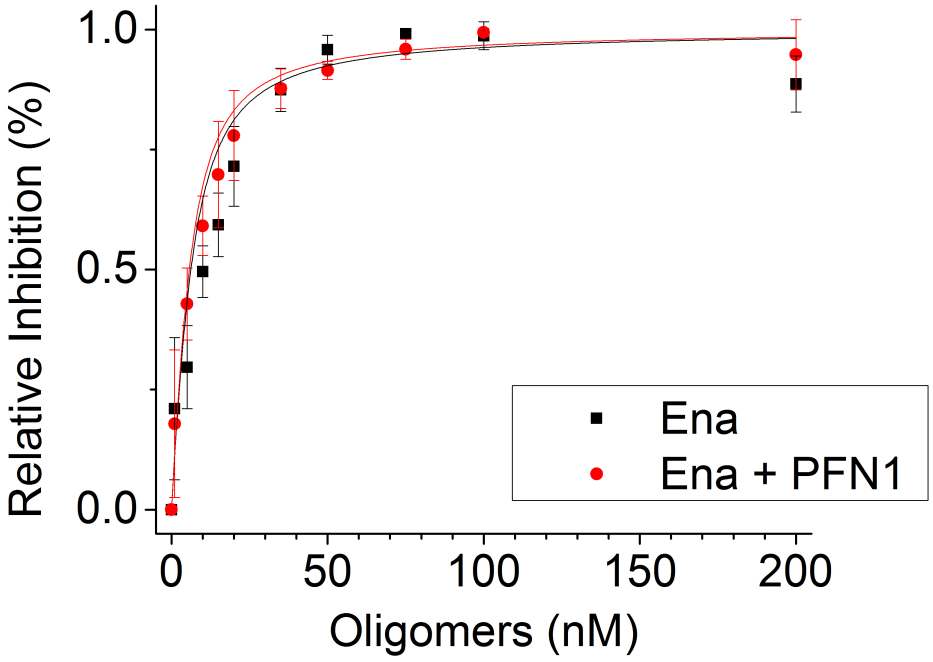

Figure 6: Isotherm binding plot of various oligomer concentrations on polymerization of 2.5 µM actin mediated by 20 nM Ena(ΔL) in the absence and presence of PFN1. The resulting IC_{50} values were 3.70 ± 0.95 nM and 3.21 ± 0.53 nM in the absence and presence of PFN1, respectively.

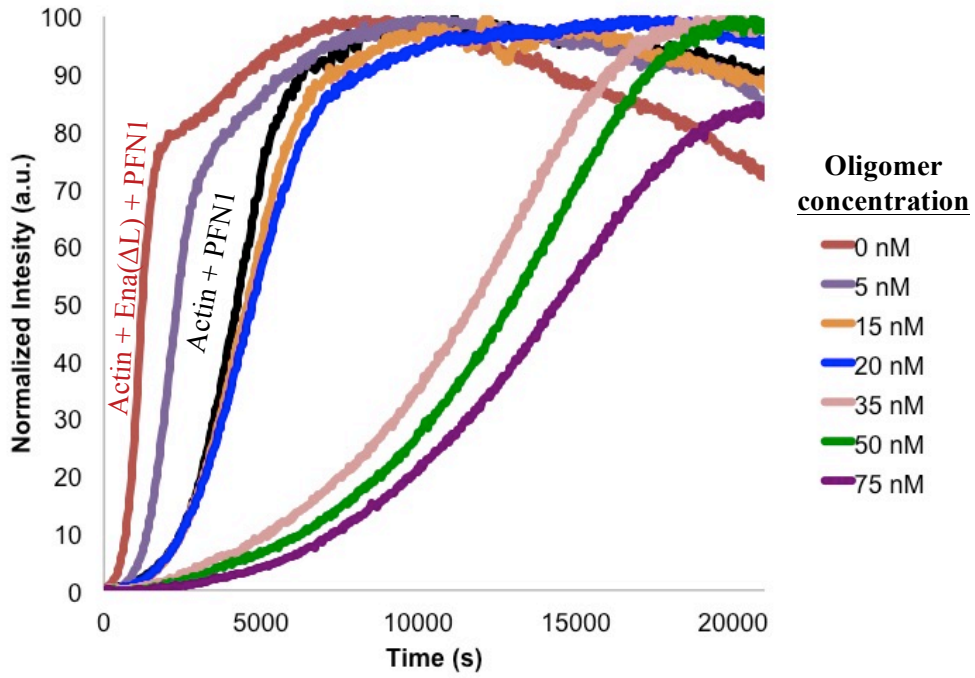

Figure 7: Effects of various oligomer concentrations on polymerization of 2.5 µM actin mediated by 20 nM Ena(ΔL) in the presence of 5 µM PFN1.

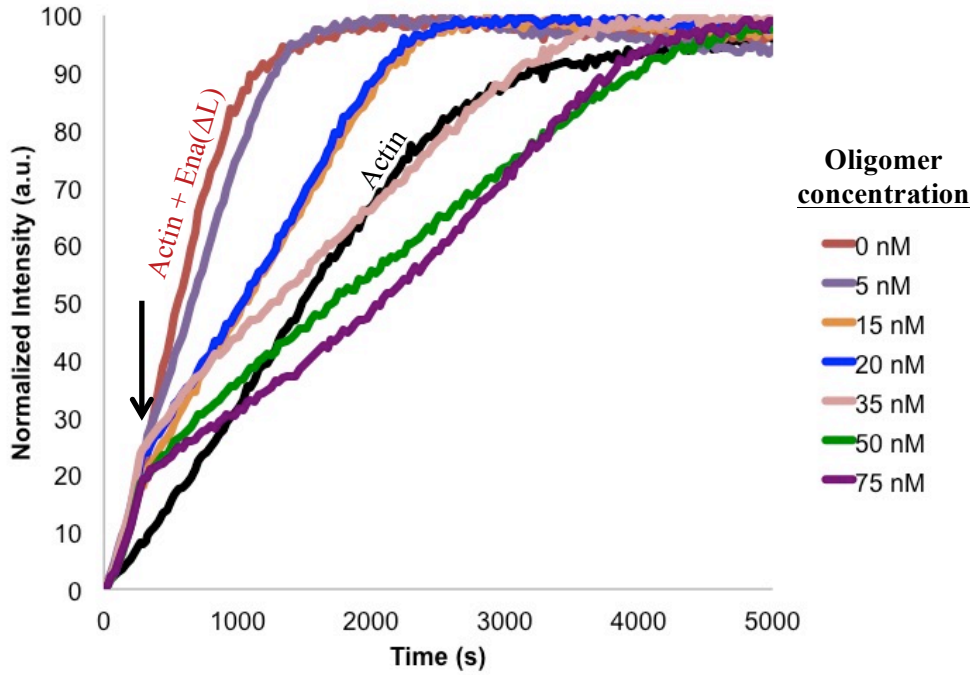

Figure 8: Effects of various oligomer concentrations on seeds that were generated by incubation of 2.5 µM actin in the presence of 20 nM Ena(ΔL). Polymerization was initiated with physiological salt concentrations and oligomers were added after ~200 s (black arrow).

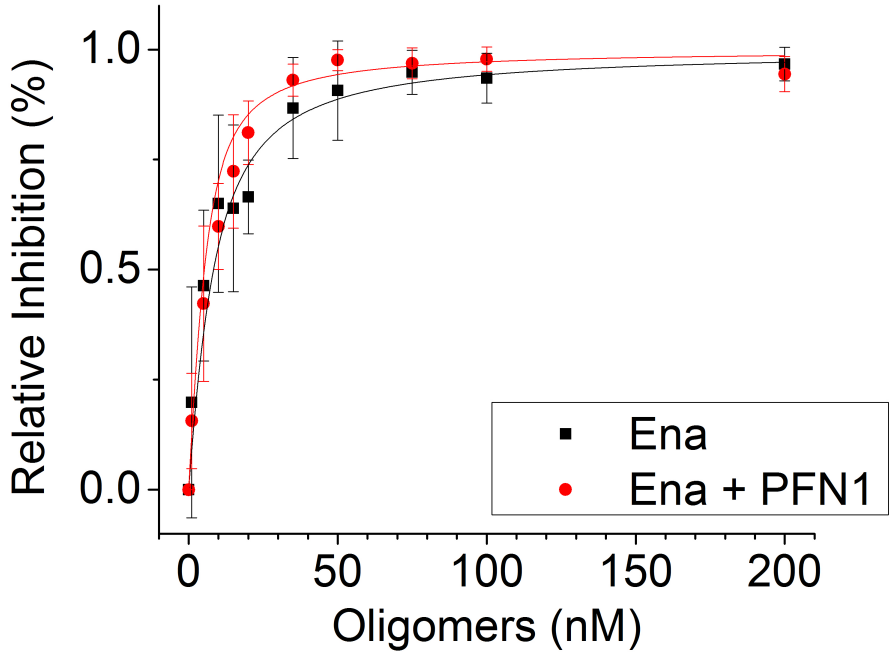

Figure 9: Isotherm binding plot of various oligomer concentrations on seeded polymerization of 2.5 μM actin mediated by 20 nM Ena(ΔL) in the absence and presence of PFN1. The resulting IC_{50} values were 5.80 ± 0.69 nM and 2.73 ± 0.45 nM in the absence and presence of PFN1, respectively.

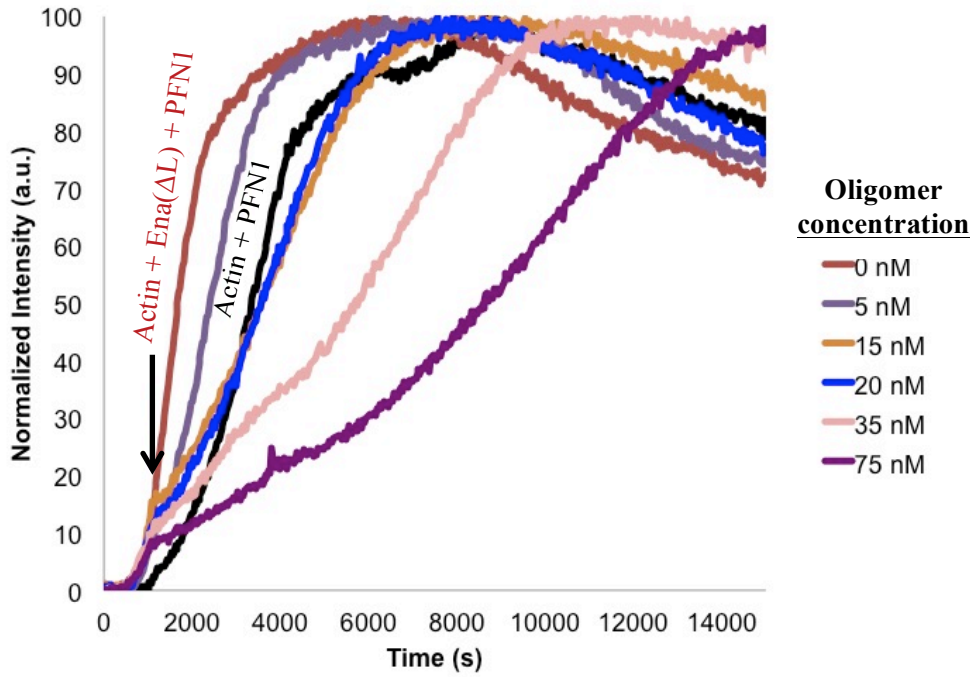

Figure 10: Effects of various oligomer concentrations on seeds that were generated by incubation of 2.5 μM actin in the presence of 20 nM Ena(ΔL) and 5 μM PFN1. Polymerization was initiated with physiological salt concentrations and oligomers were added after ~960 s (black arrow).

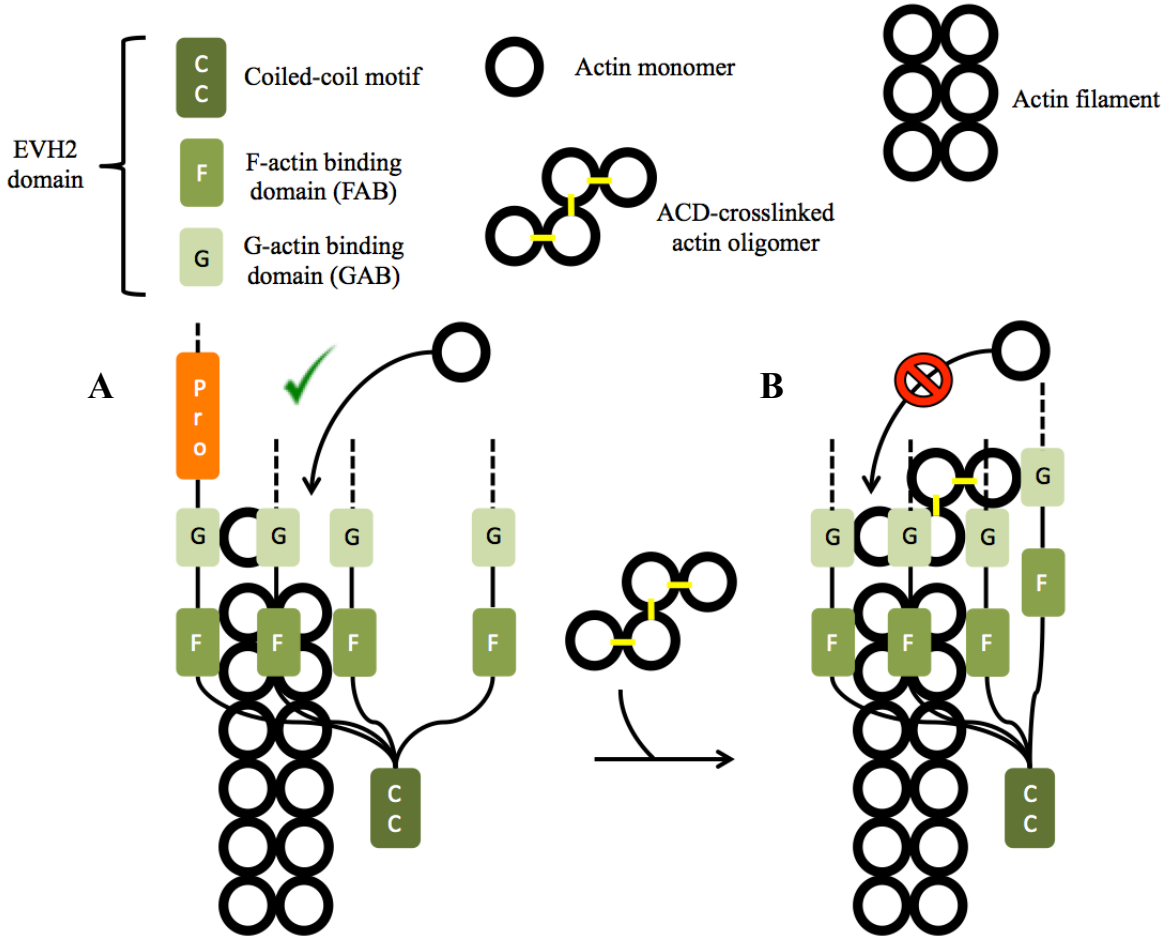

Figure 11: The proposed mechanism of Ena inhibition by the ACD-crosslinked actin oligomers. **A)** The EVH2 domain of Ena(ΔL) processively binds to a growing barbed end of an actin filament and accelerates filament elongation. Additional monomers can get incorporated through interactions with the GAB domain and subsequent binding to the filament. **B)** Once the ACD-crosslinked actin oligomer binds to multiple GAB domains on Ena(ΔL), additional monomers cannot be added to the filament. The addition of the oligomer has turned Ena(ΔL) into a capping protein. We believe that oligomer binding to multiple GAB domains simultaneously provides the basis for its potency.

6. References

1. Yamaizumi M, Mekada E, Uchida T, Okada Y. One molecule of diphtheria toxin fragment a introduced into a cell can kill the cell. Cell. 1978 Sep 1;15(1):245–50.

2. Richard JF, Petit L, Gibert M, Marvaud JC, Bouchaud C, Popoff MR. Bacterial toxins modifying the actin cytoskeleton. Int Microbiol Off J Span Soc Microbiol. 1999 Sep;2(3):185–94.

3. Aktories K, Lang AE, Schwan C, Mannherz HG. Actin as target for modification by bacterial protein toxins. FEBS J. 2011 Dec 1;278(23):4526–43.

4. Goldberg MB. Actin-Based Motility of Intracellular Microbial Pathogens. Microbiol Mol Biol Rev. 2001 Dec 1;65(4):595–626.

5. Desouza M, Gunning PW, Stehn JR. The actin cytoskeleton as a sensor and mediator of apoptosis. Bioarchitecture. 2012 May 1;2(3):75–87.

6. Blanchoin L, Boujemaa-Paterski R, Sykes C, Plastino J. Actin Dynamics, Architecture, and Mechanics in Cell Motility. Physiological Reviews. 2014 Jan 1;94(1):235–63.

7. Wickramarachchi D, Theofilopoulos AN, Kono DH. Immune Pathology Associated with Altered Actin Cytoskeleton Regulation. Autoimmunity. 2010 Feb;43(1):64–75.

8. Welch MD, Rosenblatt J, Skoble J, Portnoy DA, Mitchison TJ. Interaction of human Arp2/3 complex and the Listeria monocytogenes ActA protein in actin filament nucleation. Science. 1998 Jul 3;281(5373):105–8.

9. Heisler DB, Kudryashova E, Grinevich DO, Suarez C, Winkelman JD, Birukov KG, et al. ACD toxin-produced actin oligomers poison formin-controlled actin polymerization. Science. 2015 Jul 31;349(6247):535–9.

10. Kudryashov DS, Durer ZAO, Ytterberg AJ, Sawaya MR, Pashkov I, Prochazkova K, et al. Connecting actin monomers by iso-peptide bond is a toxicity mechanism of the Vibrio cholerae MARTX toxin. Proc Natl Acad Sci U S A. 2008 Nov 25;105(47):18537–42.

11. Kudryashov DS, Cordero CL, Reisler E, Fullner Satchell KJ. Characterization of the Enzymatic Activity of the Actin Cross-Linking Domain from the Vibrio cholerae MARTXVc Toxin. J Biol Chem. 2008 Jan 4;283(1):445–52.

12. Fullner KJ. In vivo covalent cross-linking of cellular actin by the Vibrio cholerae RTX toxin. EMBO J. 2000 Oct 16;19(20):5315–23.

13. Cordero CL, Kudryashov DS, Reisler E, Satchell KJF. The Actin Cross-linking Domain of the Vibrio cholerae RTX Toxin Directly Catalyzes the Covalent Cross-linking of Actin. J Biol Chem. 2006 Sep 5;281(43):32366–74.

14. Satchell KJF. Actin Crosslinking Toxins of Gram-Negative Bacteria. Toxins. 2009 Dec 1;1(2):123–33.

15. Kudryashova E, Kalda C, Kudryashov DS. Glutamyl Phosphate Is an Activated Intermediate in Actin Crosslinking by Actin Crosslinking Domain (ACD) Toxin. PLoS One. 2012 Sep 21;7(9).

16. Breitsprecher D, Goode BL. Formins at a glance. J Cell Sci. 2013 Jan 1;126(1):1–7.

17. Pollard TD. Actin and Actin-Binding Proteins. Cold Spring Harb Perspect Biol. 2016 Mar 17;a018226.

18. Matthias Krause, Erik W. Dent, James E. Bear, Joseph J. Loureiro, Gertler and FB. Ena/VASP Proteins: Regulators of the Actin Cytoskeleton and Cell Migration. Annu Rev Cell Dev Biol. 2003;19(1):541–64.

19. Winkelman JD, Bilancia CG, Peifer M, Kovar DR. Ena/VASP Enabled is a highly processive actin polymerase tailored to self-assemble parallel-bundled F-actin networks with Fascin. Proc Natl Acad Sci U S A. 2014 Mar 18;111(11):4121–6.

20. Ahern-Djamali SM, Comer AR, Bachmann C, Kastenmeier AS, Reddy SK, Beckerle MC, et al. Mutations in Drosophila enabled and rescue by human vasodilator-stimulated phosphoprotein (VASP) indicate important functional roles for Ena/VASP homology domain 1 (EVH1) and EVH2 domains. Mol Biol Cell. 1998 Aug;9(8):2157–71.

21. Ball LJ, Jarchau T, Oschkinat H, Walter U. EVH1 domains: structure, function and interactions. FEBS Lett. 2002 Feb 20;513(1):45–52.

22. Ferron F, Rebowski G, Lee SH, Dominguez R. Structural basis for the recruitment of profilin–actin complexes during filament elongation by Ena/VASP. EMBO J. 2007 Oct 31;26(21):4597–606.

23. Bachmann C, Fischer L, Walter U, Reinhard M. The EVH2 Domain of the Vasodilator-stimulated Phosphoprotein Mediates Tetramerization, F-actin Binding, and Actin Bundle Formation. J Biol Chem. 1999 Aug 13;274(33):23549–57.

24. De La Cruz EM, Ostap EM, Brundage RA, Reddy KS, Sweeney HL, Safer D. Thymosin-beta(4) changes the conformation and dynamics of actin monomers. Biophys J. 2000 May;78(5):2516–27.

25. Trichet L, Sykes C, Plastino J. Relaxing the actin cytoskeleton for adhesion and movement with Ena/VASP. J Cell Biol. 2008 Apr 7;181(1):19–25.

26. Cooley L, Verheyen E, Ayers K. chickadee encodes a profilin required for intercellular cytoplasm transport during Drosophila oogenesis. Cell. 1992 Apr 3;69(1):173–84.

27. Spudich JA, Watt S. The Regulation of Rabbit Skeletal Muscle Contraction I. BIOCHEMICAL STUDIES OF THE INTERACTION OF THE TROPOMYOSIN-

TROPONIN COMPLEX WITH ACTIN AND THE PROTEOLYTIC FRAGMENTS OF MYOSIN. J Biol Chem. 1971 Aug 10;246(15):4866–71.

28. Kudryashova E, Heisler D, Zywiec A, Kudryashov DS. Thermodynamic properties of the effector domains of MARTX toxins suggest their unfolding for translocation across the host membrane. Mol Microbiol. 2014 Jun 1;92(5):1056–71.

29. Lu J, Pollard TD. Profilin Binding to Poly-l-Proline and Actin Monomers along with Ability to Catalyze Actin Nucleotide Exchange Is Required for Viability of Fission Yeast. Mol Biol Cell. 2001 Apr 1;12(4):1161–75.

30. Kuhn JR, Pollard TD. Real-Time Measurements of Actin Filament Polymerization by Total Internal Reflection Fluorescence Microscopy. Biophys J. 2005 Feb;88(2):1387–402.